**Smart Structures and Systems**, *Vol. 17, No. 2 (2016) 313-325*
DOI: http://dx.doi.org/10.12989/sss.2016.17.2.313 

# An approach to design and fabrication of resonant giant magnetostrictive transducer

Mohammad R. Sheykholeslami[1], Yousef Hojjat*[2], Simone Cinquemani[3], Mojtaba Ghodsi[4] and M. Karafi[2]

*[1]Department of Mechanical Engineering, Faculty of Engineering, Arak University, Arak, Iran*
*[2]Mechanical Eng., Dep., Tech and Eng. Faculty, Tarbiat Modares University, Iran*
*[3]Department of Mechanical Engineering, Politecnico di Milano, Milan, Italy*
*[4]Mechanical and Industrial Eng., Dep., College of Eng. Sultan Qaboos University, Oman*

*(Received March 25, 2015, Revised December 7, 2015, Accepted December 20, 2015)*

**Abstract.** The paper provides a comprehensive procedure for the mechanical and magnetic design of Langevin transducer based on giant magnetostrictive material. The the transducer is designed to work at its second mode of vibration, having high mechanical quality factor and low damping coefficient. The design procedure is based on an analytical model and it is verified by finite-element analysis. Experimental tests based on impedance response analysis in first and second modes are carried out on the prototype. Results confirm the appropriate design of this transducer, demonstrating the highest mechanical quality factor between the resonant transducers in the literature.

**Keywords:** magnetostrictive; terfenol-D; resonant transducer; mechanical quality factor

## 1. Introduction

Magnetostriction is changing shape of ferromagnetic materials under the influence of an external magnetic field (Sheykholeslami *et al.* 2016). This property of some metals and alloys is widely used in solid state transducers. Some of these materials, called giant magnetostrictive materials, exhibit high strain and high energy density. Terfenol-D is the most widespread magnetostrictive material and it is an alloy of Ferrous, Terbium and Dysprosium that was initially developed in the 1970s to be used in sonar systems (Claeyssen *et al*. 1988). Various kinds of Terfenol-D actuators are presented for static and semi-static operations. As an example, Wang Lee et.al presented a design procedure of Terfenol-D actuator based on the use of a permanent magnet in 2007 (Wang *et al.* 2010). Grunwald et.al reviewed design considerations of magnetostrictive actuator in 2008 (Grunwald and Olabi 2008). Karanadehi *et al*. in 2010 presented an actuator and used it in high dynamics servo valve (Karunanidahi and Singaperumal 2010).

Resonant transducers are characterized by higher displacement than static and quasi-static devices as they operate in their resonant frequency (Sheykholeslami *et al.* 2015). A parameter to evaluate the performance of these transducers is their mechanical quality factor. It is defined as the

*Corresponding author, Professor, E-mail: yhojjat@modares.ac.ir


http://www.techno-press.org/?journal=sss&subpage=8 ISSN: 1738-1584 (Print), 1738-1991 (Online)

ratio between the displacement of the tip of the device in resonance frequency and the static displacement (Sheykholeslami *et al*. 2015). According to scientific literature, this ratio is between 3 to 20 for Terfenol-D alloy (Olabi and Grunwald 2008).

There are some works related to the design of resonance magnetostrictive transducers. Dhishla et.al in 1997 introduced a low frequency giant magnetostrictive material transducer that resonates at a frequency of 3.1 kHz in air and 2.65 kHz in water with a quality factor of 6 (Dilsha *et al*. 1997). Son and Chao in 1997 used the Terfenol-D transducer for sonar application. Calculated resonance frequency of this transducer is 2.5 kHz and actual resonance frequency is 2.1 kHz (Son and Cho 1999). Wenjing et.al reported a comparison study between piezoelectric and Terfenol-D transducers for use at higher operating frequencies (about 15 kHz). This study showed some advantages of Terfenol-D transducer such as low applied voltage, higher power density and lower impedance (Wenjing *et al*. 2006). The design and fabrication procedure of a giant magnetostrictive composite transducer, whose working frequency is 64 kHz, is reported in (Wing *et al.* 2006). The mechanical quality factor of this transducer is 39.6 and effective coupling factor is 0.21. Quality factor of its composite value is about 30. Karafi et.al introduced resonance hybrid longitudinal-torsional magnetostrictive transducer (Karafi *et al*. 2013). Ductile magnetostrictive material was used for fabricating this transducer with a configuration different from the Langevin's one. Sheykholeslami et. al studied the effect of Young modulus change on the behavior of a giant magnetostrictive transducer (Sheykholeslami *et al*. 2015) showing such effects can be neglected when the device works at its second mode of vibration.

According to the state of the art in this field, it is clear that there is no a clear and effective approach to the design and optimization of giant magnetostrictive resonant actuators.

This work introduces a design procedure to develop Terfenol-D transducer for working at 8.25 kHz with very high mechanical quality factor. The paper introduces all the steps to the design of these devices and demonstrates that, by insulating the mechanical pre-load mechanism and the magnetic bias system from vibrating parts of the transducer, it is possible to greatly increase the performance of the device.

The paper is structured as follows. Section 2 describes the design procedure of the transducer, especially from mechanical and magnetic points of view. Performance analysis of the device is introduced in section 3. Section 4 discusses results from the experimental tests carried out on the prototype. Results show that the new device has a quality factor considerably higher than all the others described in the literatures. Finally conclusions are drawn is Section 5.

## 2. Design procedure

Resonant transducers are used to generate sonic and ultrasonic vibration. As their name suggests, these devices should work at their resonance frequencies to enhance the amplitude of mechanical vibration. According to Fig. 1, resonant transducers have 3 main parts: excitation part (based on piezoelectric or magnetostrictive material), backing part (tail mass) and matching part (head mass).

Terfenol-D can be profitably used for these devices and should be suitably magnetically and mechanically pre-loaded to increase the efficiency of the transducer (Calkins *et al*. 1997). Exploiting results from previous studies, magnetic bias and mechanical pre-load have been set equal to 35~45 kA/m and 10.34 MPa respectively.

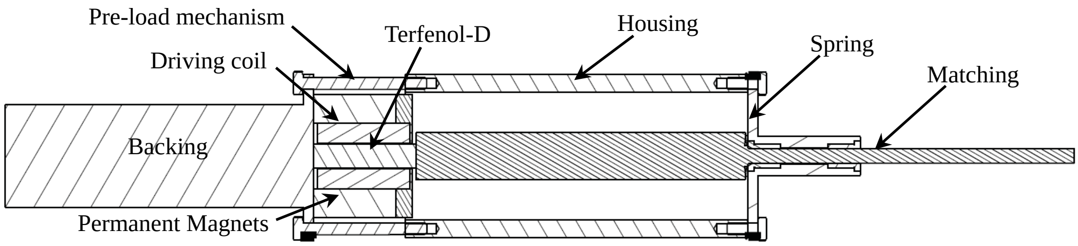


Fig. 1 Layout of a Magnetostrictive resonant transducer

Selection criteria for backing and matching materials are:

1. Acoustic impedance relationship between the main parts should satisfy Eq.(1) (Amir *et al.* 2007)

$$Z_t = \sqrt{Z_b Z_m} \tag{1}$$

   where the acoustic impedance $Z$ is the product between the density of the material and the sound velocity through it ($Z_t$ is related to Terfenol-D, $Z_b$ to the backing part and $Z_m$ to the matching one).
2. Backing should be ferromagnetic to cope with magnetic design (see par 2.1).
3. Density of the backing material should be high enough.
4. Fatigue strength of the matching should be high enough.
5. Elongation of the matching materials should be as high as possible.
6. Backing and matching materials should have a high heat conductivity coefficient in order to facilitate heat dissipation.

Considering above restrictions, stainless steel 420 for the backing and aluminum 7075 for the matching have been selected. To calculate the resonant length of each part, density and sound velocity of materials have to be precisely determined. These properties are experimentally obtained and shown in Table 1.

Young modulus ($E$) and Poisson ratio ($\upsilon$) can be measured by acoustic methods. By measuring sound wave speed in materials along longitudinal and transversal directions. $E$ and $\theta$ can be obtained by the following equations (Krautkramer and Krautkramer 1990)

Table 1 Mechanical properties of the materials

| Material | Young Modulus(GPa) | Poisson Ratio | Sound Velocity($ms^{-1}$) | Density($kg\ m^{-3}$) |
|---|---|---|---|---|
| Terfenol-D | 40 | 0.35 | 3450 | 9000 |
| Aluminum | 77 | 0.33 | 6330 | 2823 |
| Stainless steel 420 | 200 | 0.285 | 6050 | 7550 |

$$E = \frac{\rho\, C_s (3C^2 - 4C_s^2)}{(C^2 - C_s^2)} \tag{2}$$

$$\upsilon = \frac{1 - 2(\frac{C_s}{C})^2}{2(1 - \left(\frac{C_s}{C}\right)^2)} \tag{3}$$

where ρ is the density and $C$ and $C_s$ are longitudinal and shears sound wave velocities in the material. $C$ and $C_s$ are measured by pulse-echo method using ultrasonic probe (Krautkramer and Krautkramer 1990). By measuring time of path travelling (time between two peaks), sound velocity is given by Eq. (4).

$$C = \frac{L_{wave}}{t} \tag{4}$$

where $L_{wave}$ is the length of pulse traveling path and t is the corresponding time. Shear velocity is measured with the same procedure, but analyzing shear pulse in materials.

According to (Markov 1966), main dimensions of backing and matching parts can be obtained from Eq. (5)

$$\frac{d^2a}{dx^2} + \frac{1}{A}\frac{dA}{dx}\frac{da}{dx} + \frac{\omega^2}{C^2}a = 0 \tag{5}$$

where A is the cross section area of each part, a is vibration amplitude, $\omega$ is resonance frequency (designed equal to 8 kHz) and $C$ is sound velocity. Coordinate $x$ is shown in Fig. 2.

If main parts of the transducer are divided into 5 parts, Eq. (5) should be satisfied along them. As each part has constant cross section area, the term dA/dx is equal to zero. Thus, Eq. (5) can be rewritten as

$$\frac{d^2a}{dx^2} + \frac{\omega^2}{C^2}a = 0 \tag{6}$$

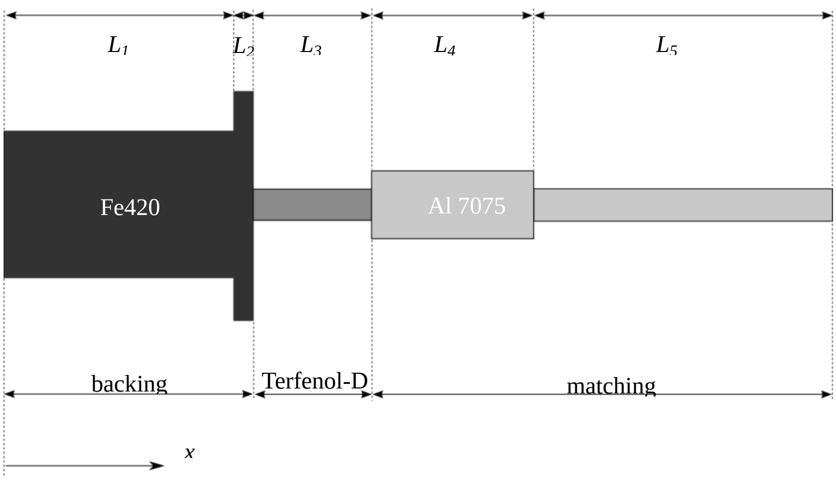


Fig. 2 Main parts of the transducers and corresponding lengths

Table 2 Transducer main dimensions

| Main part | Length [mm] | Diameter [mm] |
|---|---|---|
| Backing | 15 | 50 |
| Terfenol-D | 5 | 10 |
| Matching | 15.75 | 23 |
| | 15.75 | 7 |

Boundary conditions for solving Eq. (6) are the equalities of force and amplitude in the interface planes of main parts. Also, two ends of the transducer are free, hence force in these points is equal to zero. A detailed explanation of analytical approach can be found in (Sheykholeslami *et al.* 2015).

Matching is considered to be step shaped to obtain maximum output vibration amplitude. As it is shown in Fig. 2, step shaped matching has two cross sections. Amplification factor in this shape is proportional to the ratio of these two cross section areas. Eq. (7) shows relationship for the amplification factor *AF* for step shaped matching

$$\mathrm{AF} = \left(\frac{D_1}{D_2}\right)^2 \tag{7}$$

Where $D_1$ is the diameter of the larger cross section and $D_2$ is the diameter of the smaller one. In this paper, this factor is set equal to 10. In selecting each part of the transducer diameter, there are two restrictions. First, in order to prevent disturbing shear and lateral modes of vibration, diameter of each part should be smaller than $\lambda_i/2$ ($\lambda_i$ is acoustic wavelength in each part of the transducer). Second, in order to approximate sound velocity by $(E/\rho)^{1/2}$ for solving Eq. (6), diameters of each part should be smaller than $\lambda_i/4$ (Amir *et al*. 2007). Considering these restrictions, the diameter of Terfenol-D is selected to be 10 mm. For matching part, by considering amplification factor, diameter of the larger cross section area is selected to be 23 mm and the smaller cross section diameter is 7 mm. Backing should be part of the magnetic circuit therefore its dimensions depend also on the magnetic design (see. Par. 2.1).

An interesting innovative aspect of the design of this device is that the pre-stress mechanism and the magnetic circuit components are placed at nodes of vibration not to affect the dynamics of the transducer and to maximize the energy transmitted to the matching part. This innovative aspect is crucial to obtain high performance and represents a step forward in the design of resonant transducers. Moreover, this new configuration allows to have constant mechanical pre-load of Terfenol-D during operation, thus increasing its fatigue life.

Eq. (6) can be solved for each of the five parts of the transducer and lengths of each part are obtained. Table 2 resumes their main dimensions.

A finite element analysis has been carried out to check the position of nodes, according to the mechanical design of the transducer. Fig. 3 shows the modal shape of the second mode of the transducer. As shown, nodes are located at the same place as determined in the theoretical design and the desired amplification factor (*AF*) is obtained. Resonance frequency is 8020 Hz, which is in good agreement with the theoretical design.

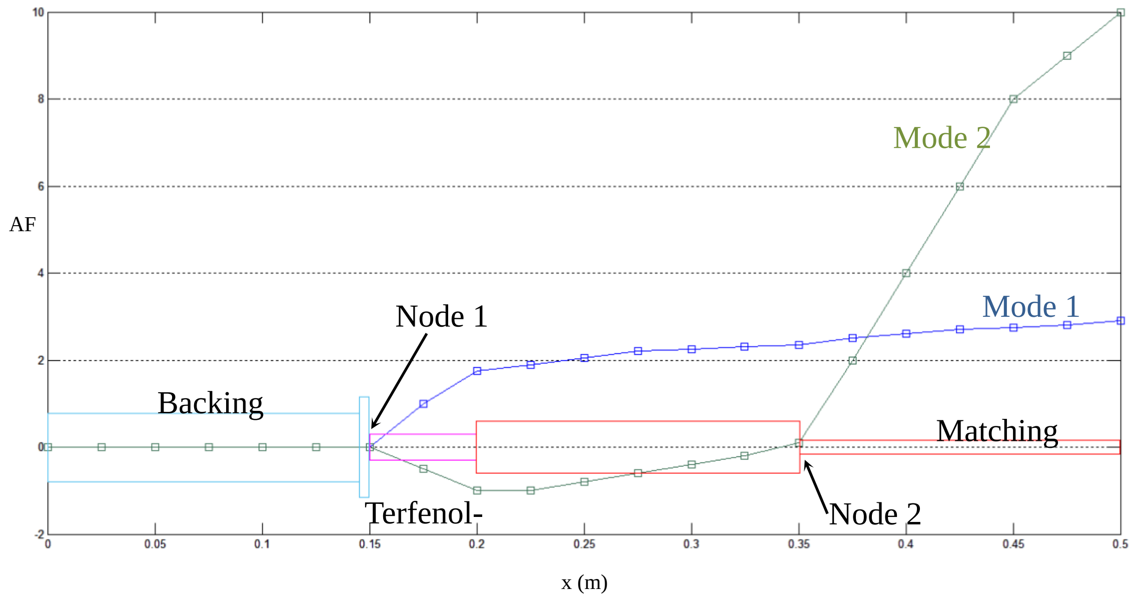


Fig. 3 First and second modal shape of the transducer obtained from finite element analysis

### *2.1 Magnetic design*

The purpose of magnetic design is to provide magnetic bias field and excitation field in Terfenol-D, paired with a low reluctance magnetic circuit. Permanent magnets are selected for bias field instead of using a coil with DC current to avoid heating of Terfenol-D that would affect its performance. Main alternatives are NdFeB and ceramic permanent magnets. Table 3 shows main properties of these permanent magnets.

Numerical analysis have been carried out to evaluate the magnetic bias field throughout the magnetostrictive material. In this simulation, it is considered that enough magnetic bias fields have been generated in Terfenol-D. Results show that the ceramic ring shaped permanent magnet (PM) with 30 mm inner diameter and 60 mm outer diameter generates the appropriate bias field. For a proper magnetic circuit, backing is made of magnetic steel and a high permeability 80 mm diameter coupler is added (Fig. 4). Constrains discussed in par. 2.1 leads to design main part of backing with a 50mm diameter (Table 2).

Table 3 Permanent magnets properties

| Magnetic Material | Grade | Br(T) | Hc(A $m^{-1}$) | $(BH)_{max}$(T A $m^{-1}$) |
|---|---|---|---|---|
| NdFeB | 39H | 1.28 | 978803 | 1252868 |
| NdFeB | B110N | 0.68 | 459957 | 312771 |
| Ceramic | 8 | 0.39 | 254648 | 99313 |

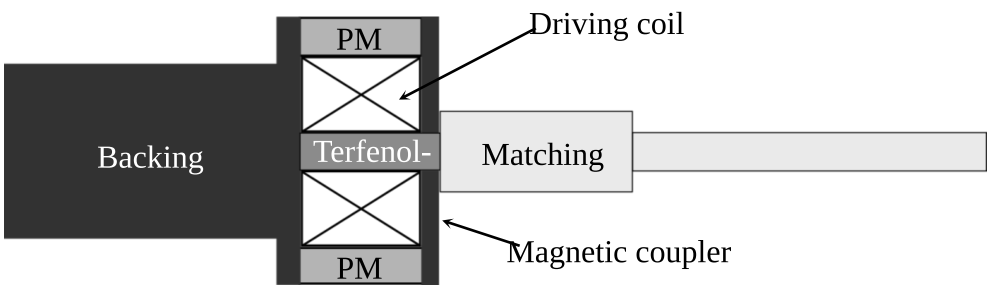


Fig. 4 The magnetic circuit of the transducer

Fig. 5 shows magnetic flux density in the centerline of the magnetic circuit using the ceramic permanent magnet. Figure 6 shows magnetic flux density versus magnetic field in Terfenol-D with 10.34 MPa mechanical pre-load. Mean flux density in Terfenol-D due to ceramic permanent magnets is approximately 0.4 T, corresponding to a 40 kA/m magnetic bias fields (Fig. 6).

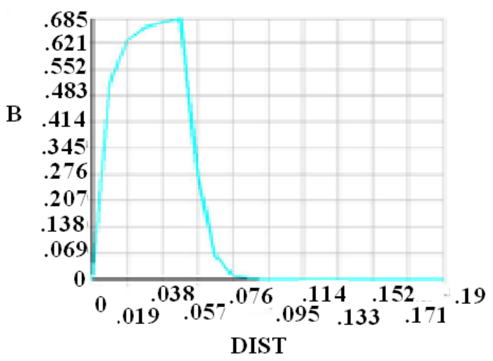


Fig. 5 The magnetic flux density across the magnetostrictive rod due to permanent magnets

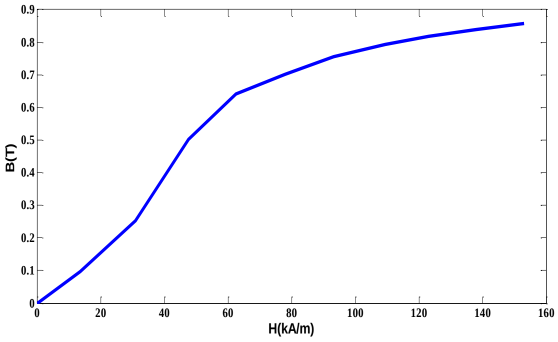


Fig. 6 The magnetic flux density versus magnetic field intensity with 10.34 MPa pre-load

## 3. Performance analysis

The performance of a resonant transducer can be evaluated through two main indices: the quality factor and the speed of the tip per input current.

A common way to get these indices is to model the transducer as an ideal gyrator (see Fig. 7) by using impedance data (Engdahl 2000). Eq. (8). This gyrator convert electrical to mechanical energy and vies versa. In magnetostrictive transducer, Gyrator coefficient is complex number, thus it is changed both amplitude and phase of input. Eq. (8) show the relationships between parameters of gyrator in two branches

$$U = Z_e I + T_{em} v \qquad (8)$$
$$F = T_{me} I + Z_m v$$

where U is the applied voltage, I is the current, v is the velocity of the transducer, $Z_e$ and $Z_m$ are the electrical and mechanical impedances of the transducer, respectively. $T_{em}$ is the electromotive force per velocity, while $T_{me}$ is the mechanical force per current.

In the mechanical resonance frequency, imaginary part of the mechanical impedance is equal to zero. According to Eq. (10), in the free state condition of the transducer (F=0), impedance of the transducer ($Z_{ee}$) is (Engdahl 2000)

$$Z_{ee} = R_{ee} + jX_{ee} = Z_e + \frac{-T_{me}T_{em}}{Z_m} = Z_e + Z_{mot} \qquad (10)$$

where $Z_{mot}$ is the motional impedance. In clamping state, this factor is zero. By knowing the impedance of the transducer in free and clamped conditions, motional impedance can be obtained. By using this data and correct resonance frequency, mechanical quality factor can be calculated. According to Fig. (11) circular region for real and imaginary parts of the motional impedance is a circle-shaped locus in the complex plane. A line orthogonal to the diameter between origin and a point related to resonance frequency crosses the circle in two points named as $\dot{\omega}$ and $\ddot{\omega}$.

Mechanical quality factor (Q factor) can be calculated as (Engdahl 2000)

$$Q_m = \frac{\omega_0}{\ddot{\omega} - \dot{\omega}} \qquad (11)$$

where $\omega_0$ is the resonance frequency.

Mechanical quality factor shows vibrational amplitude in resonance frequency compared to static condition. Higher mechanical quality factors show higher efficiency of the transducer.

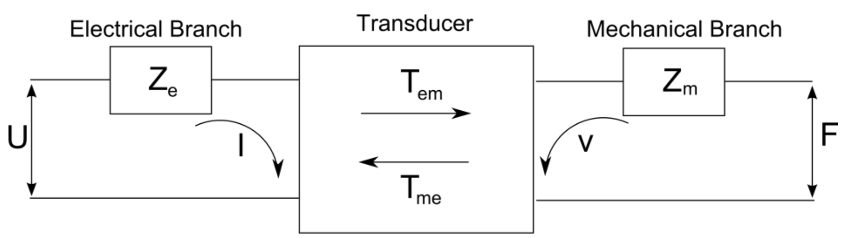


Fig. 7 The schematic model for transducer (Engdahl 2000)

Ratio of output velocity per input current ($M_m$) evaluates the effectiveness of the transducer. Exploiting Eq. (8), it can be obtained as

$$M_m = \frac{v}{I} = \frac{Z_{ee} - Z_e}{T_{em}} = \frac{Z_{mot}}{T_{em}} \tag{12}$$

## 4. The prototype

According to the design described in section 2, a prototype of the resonant transducer has been manufactured. Fig. 8 shows separate parts and assembly of the prototype. Flatness and parallelism of the parts that are connected to Terfenol-D have to be checked, as any non-axial force could cause a fracture in Terfenol-D.

The resonance frequency of the transducer can be obtained from impedance response analysis. Wayne Kerr 6500B impedance analyser is used. Fig. 9 shows the experimental setup of this test. Impedance amplitude and phase of the transducer are measured for free and blocked conditions. As it is known, a rapid change in impedance is occurred near resonance frequency (Fig. 10).

By using impedance method, quality factor can be calculated for each mode of vibration of the transducer. According to the impedance test, resonance frequency in the second longitudinal mode is 8252 Hz. Good agreement between analytical and FEM prediction for the resonance frequency can be observed (error lower than 1%).

According to Fig. (11) circular region for real and imaginary parts both in 2nd modes of vibration. By plotting the diameter between origin and correspondence resonance frequency point in this figure and also perpendicular diameter, the mechanical quality factor can be calculated. It results equal to 134.2 for the second mode. By repeat the procedure for first mode, 27.7 is obtained. It is stem from seperating main pats, because lower energy is consumed in second mode to vibrate pre-load mechanism.

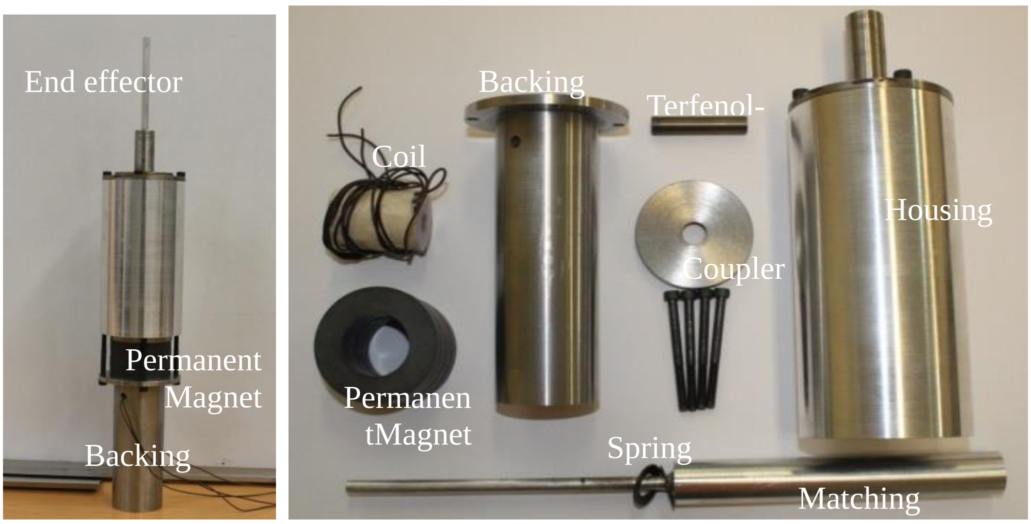


Fig. 8 The assembled transducer and its parts

Fig. 9 Setup for impedance test

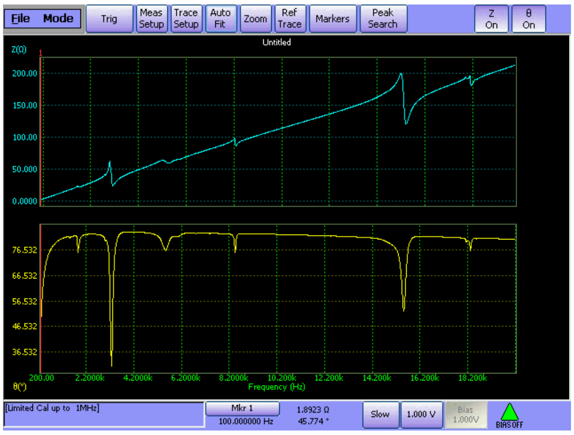

Fig. 10 Impedance response of the transducer (amplitude and phase)

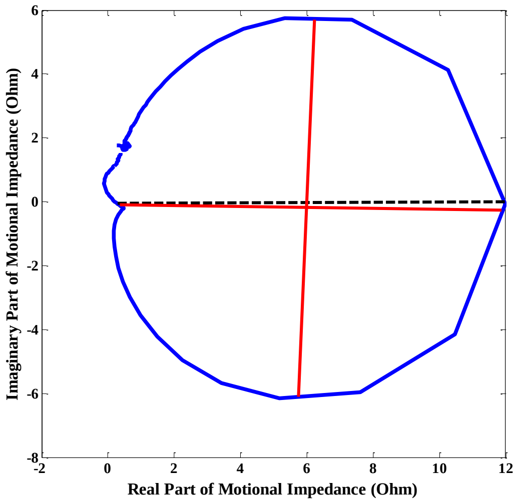


Fig. 11 Locus of motional impedance

Similar considerations can be done looking at Fig. 12 and 13 where motional impedance amplitude is depicted, as a function of frequency, for first and second mode respectively. For both operating conditions, quality factors are higher than both commercial and experimental devices, thus confirming the appropriate design from both the mechanical and the magnetic point of view.

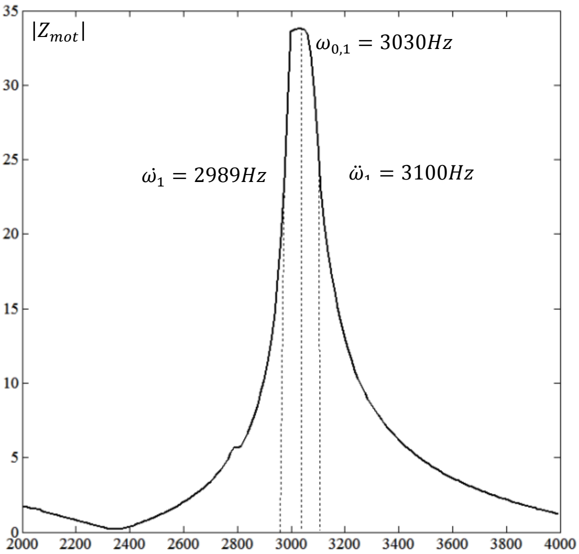


Fig. 12 Motional impedance amplitude in first mode

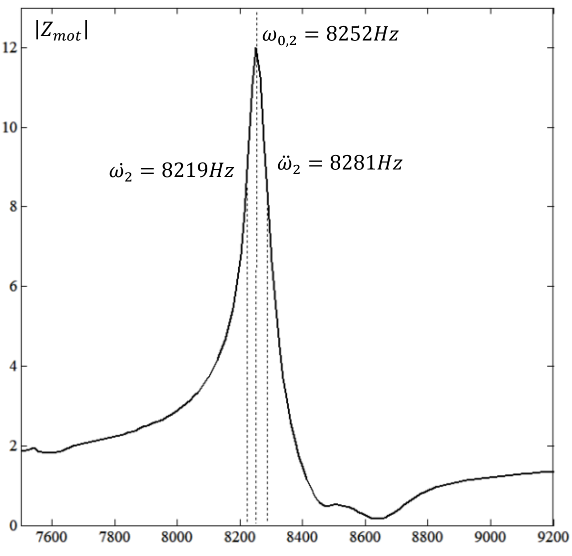


Fig. 13 Motional impedance amplitude in second mode

Table 4 Speed per input current in first and second modes

| Mode | Voltage [V] | $M_m$=v/I [mm/(s.A)] |
|---|---|---|
| 1 | 100 | 29.43 |
| 2 | 100 | 288.72 |

In particular, the result obtained in the second mode is far superior to any device described in the literature. As a matter of fact, by placing the preload mechanism in correspondence of one of the nodes, the energy dissipation has been minimized and the preload of Terfenol-D has been manteined as constant,.

Finally a test to compare performance in different operating modes is carried out measuring the output velocity per input current in first and second modes of the transducer in similar working condition (applied voltage equal to 100 V). Eddy current gap sensor (model AEC-5509 by Applied Electronic Corp.) is used to measure vibration amplitude. The sensitivity of the sensor is 0.4 mm/V. Acs 712 current sensor is used to measure input current whose sensitivity is 100 mV/A.

Table 4 shows the comparison between the two working condition in terms of speed-current ratio.

Higher value of $M_m$ in the second mode shows a higher electromechanical transformer factor ($T_{em}$) and therefore a higher effectiveness of the device in this condition.

Due to a higher quality factor and higher electromechanical transformer factor, displacement in second mode operating frequency is higher. Performance of the transducer are extremely good and quality factor obtained is the highest compared to resonant transducers described in scientific literature.

## 5. Conclusions

In this paper, design and fabrication procedure of a high performance resonant giant magnetostrictive transducer has been presented. A comprehensive approach has been adopted to optimize the effectiveness of the device. Mechanical and magnetic design have been supported by analytical and numerical approaches along with experimental tests to precisely estimate main features of the materials used. Experimental impedance response on the first prototype highlights good agreement with results from finite element analysis. Resonance frequencies are close to the designed ones and the transducer behaviour matches the design objectives. The paradigm of insulating vibrating parts from pre-load mechanism allowed to enhance the performace of the device in its second mode. This allowed to reduce energy losses and then to greatly improve the effectiveness of the device. A confirmation is the high quality factor measured in the second mode equal to 134.18. This is the highest value in literature. Finally, a constant pre-stress on Terfenol-D during operation will enhance the fatigue strength of the magnetostrictive material.

## References

Amir, A., Mohsen, S. and Abbas, P. (2007), "An approach to design a high power piezoelectric ultrasonic transducer", *J. Electroceram*, **22**(4), 369-382.

Calkins, F.T., Dapino, M.J. and Flatau, A.B. (1997), "Effect of prestress on the dynamic performance of a terfenol-D transducer", *Proceedings of the Smart Structures and Materials*, San Diego, CA, art.3041-23.

Claeyssen, F., Boucher, D. and Pohlenz, C. (1988), "Application of magnetostrictive rare earth-iron alloys to sonar transducers", *Proceedings of UDT88*, London.

Dilsha, K.R., Markandyulu, G., Subrahmanyeswara, B.V.P. and Rama Rao, K.V.S. (1997), "Design and fabrication of low frequency giant magnetostrictive transducer", *J. Alloy Compound*, **258**(1-2), 53-55.

Engdahl, G. (2000), *Handbook of Giant Magnetostrictive Material*, Royal Institute of Technology, Stockholm Sweden.

Grunwald, A. and Olabi, A.G. (2008), "Design of a Magnetostrictive (MS) actuator", *Sensor. Actuat. - A Phys.*, **144**(1), 161-175.

Karafi, M.R., Hojjat, Y. and Sassani, F. (2013), "A new hybrid longitudinal–torsional magnetostrictive ultrasonic transducer", *Smart Mater. Struct.*, **22**(6), 065013.

Karunanidahi, S. and Singaperumal, M. (2010), "Design, analysis and simulation of magnetostrictive actuator and its application to high dynamic servo valve", *Sensor. Actuat. - A Phys.*, **157**(2), 185-197.

Krautkramer, J. and Krautkramer, H. (1990), *Ultrasonic Testing of Material*, Springer-Verlag, Berlin.

Markov, A.I. (1996), *Ultrasonic machining of intractablematerials*, Iliffe Books, London.

Olabi A.G., Grunwald A. (2008), "Design and application of magnetostrictive materials", *Material & Design*, **29(2)**, 469-483.

Sheykholeslami, M., Hojjat, Y., Cinquemani, S. and Ghodsi, M. (2015), "Design and simulation of multi-resonance sonic transducer using Terfenol-D", In *SPIE Smart Structures and Materials+ Nondestructive Evaluation and Health Monitoring* (pp. 94353G-94353G). International Society for Optics and Photonics.

Sheykholeslami, M., Hojjat, Y., Ghodsi, M. and Cinquemani, S. (2015), "Comparative discussion between first and second modes of Terfenol-D transducer", In *SPIE Smart Structures and Materials+ Nondestructive Evaluation and Health Monitoring* (pp. 94353H-94353H). International Society for Optics and Photonics.

Sheykholeslami, M., Hojjat, Y., Ghodsi, M., Kakavand, K. and Cinquemani, S. (2015), "Investigation of ΔE effect on vibrational behavior of giant magnetostrictive transducers", *J. Shock Vib*.

Sheykholeslami, M., Hojjat, Y., Ghodsi, M., Zeighami, M. and Kakavand, K. (2016), "Effect of magnetic field on mechanical properties in Permendur", *Mater. Sci. Eng.*, **651**, 598-603.

Son, D. and Cho, Y. (1999), "Under water sonar transducer using terfenol-D magnetostrictive material", *J. Magnetics*, **4**(3), 98-101.

Wang, L., Tan, J.B. and Zhang, S. (2010), "A giant magnetostrictive actuator based on use of permanent magnet", *Int. J. Adv. Manufact. Technol.*, **46**(9-12), 893-897.

Wenjing, L., Zhou, L. and Xia, T. (2006), "Rare earth ultrasonic transducer technique research", *Proceedings of the Ultrasonic2006*.

Wing, S.O., Young, C.S. and Yin, L.C. (2006), "A 64-kHz sandwich transducer fabricated using psedo 1-3 magnetostictive composite", *IEEE T. On Magnetic*, **42**(1), 47-50.

*FC*